Sustainable Energy Technologies and Assessments 40 (2020) 100746

Contents lists available at ScienceDirect

Sustainable Energy Technologies and Assessments

journal homepage: www.elsevier.com/locate/seta

Original article

Biodiesel substitution in a J69 aeronautic turbine engine: An experimental assessment of the effects on energy efficiency, technical performance and emissions

Gabriel Talero[a], Camilo Bayona-Roa[a,*], Vladimir Silva[a], Manuel Mayorga[b], Juan Pava[c], Mauricio Lopez[d]

[a] Universidad ECCI, Grupo de Investigación en Aprovechamiento Tecnológico de Materiales y Energía – GIATME, Cra. 19 No. 49-20, Bogotá 111311, Colombia
[b] Universidad Nacional de Colombia - Sede Bogotá, Facultad de Ingeniería, Departamento de Ingeniería Quimica y Ambiental, Grupo de Investigación en Procesos Quimicos y Bioquímicos, Cra. 30 No 45A-03 Edificio 412, Lab. Intrum, Bogotá, Colombia
[c] Escuela de Postgrados de la Fuerza Aérea Colombiana, Grupo de Investigación en Electrónica y Tecnologías para la Defensa – TESDA, Cra. 57 No. 43-28 – Can puerta 8, Bogotá 111321, Colombia
[d] Fuerza Aérea Colombiana, Cra. 57 No. 43-28 – Can puerta 8, Bogotá 111321, Colombia

ARTICLE INFO

Keywords:
biodiesel FAME
Jet A1
Fuel blend
J69 aircraft engine
Aviation
Energy performance

ABSTRACT

Biodiesel has been widely considered as an alternative fuel for aircraft and power generation turbine engines, but experimentation in literature is mostly limited to microturbines and technological challenges remain open regarding its sustainability. The present study publishes the experimental methodology and the obtained results of testing a full-scale turbojet engine J69-T-25A using blends of JetA1 and palm oil biodiesel with volume contents from 0% to 50%. An increased biodiesel FAME substitution and extended data analysis yields new findings. Biodiesel substitution up to 50% v/v drops the thrust force by 26,6% and raises the fuel consumption by 10,8%, causing a detriment in the efficiency near 76,3%. Albeit poor atomization is noticed, the rise in the excess air of combustion diminishes the CO and HC emissions. An optimum trade-off value of 15,8% of biodiesel volume content is found to avoid a significant reduction of efficiency and acceleration time, driving to a slight reduction in the GHG-emissions and a raise of 25% in the fuel costs. The employment of a biodiesel content above 30% harms the ignition at the start-up procedure of the engine and fosters cloudiness development at the exhaust gases during the shutdown.

Introduction

Aviation is one of the foremost energy-consuming sectors that strongly contributes to global Greenhouse Gas - GHG emissions and that is largely vulnerable to the availability and cost of fossil fuels. During 2017, the domestic and international aviation transport consumed almost 12,8% of the transport energy in the world [1] and exhaled globally over 170 million tons of CO_2 [2]. This mode of transport depends almost entirely on fossil fuels such as jet/kerosene, diesel, and gasoline, which is translated into a global oil consumption of 340 million tons of equivalent oil in 2018 with an expected increase in 3,5% per year by 2030 [3]. Remarkably, the increasing freight-transport activities throughout the world contrast with the low utilization of renewable energies in the aircraft powertrain splits.

Fortunately, a variety of alternatives to ensure a sustainable operation of the industry are to be disclosed, such as those including new modifications to the engine designs or the substitution of conventional fuels with alternative fuels [4]. Most efforts in recent years have been focused on the promotion of fossil fuel substitution by biomass-derived fuels and the study of new bio-jet fuels production pathways [5,6]. However, the participation of biofuels in the global transport fuel market is scarce and it still represents $<$ 3% of fossil fuel consumption [1]. A greater effort on the promotion of partial or total substitution of petroleum by-products in this sector becomes necessary, in the sense of new technological developments that make it feasible for the aviation industry. Indeed, the aviation biofuels are economically and ecologically sustainable since the feedstock for biofuels is available worldwide (with an expected contribution of 30% consumption arising from bio-jet fuels by 2030) [4]. Furthermore, most biofuels fit the technical specifications of the properties of conventional fuels [7], allowing the operation of engines with reduced particle emissions and similar performance when using biofuels blends [8,9].

* Corresponding author.
E-mail address: cbayonar@ecci.edu.co (C. Bayona-Roa).

https://doi.org/10.1016/j.seta.2020.100746
Received 17 February 2020; Received in revised form 8 May 2020; Accepted 24 May 2020

Nomenclature

Symbol	**Definition (Units)**
$\%EA$	Percent excess combustion air (% g/g)
A_t	Air inlet duct cross-sectional area (m^2)
P_f	Fuel pressure (kPa)
X_{CO_2}	Carbon dioxide volume content in flue gas (% v/v_e)
X_{CO}	Carbon monoxide volume content in flue gas (% v/v_e)
$\dot{m}$	Mass flow (g/s)
t_{ac}	Acceleration time (s)
w_{BD}	Biodiesel volume content in fuel blend (% v/v)
θ_{atom}	Atomization angle with fuel blend (°)
ρ_0	Density of intake air (kg/m^3)
ω_{shaft}	Main shaft rotational speed (RPM)
AFR	Air/Fuel Ratio (g/g)
EGT	Exhaust gas temperature (-)
HC	Hydrocarbons volume content in flue gas (% v/v_e)
HHV	Higher heating value (MJ/kg)
M	Moisture content in fuel (% g/g)
MW	Molar mass (g/mol)
OAT	Outer Air Temperature (°C)
SOC	Specific Operating Cost per year (USD/N•year)
SGE	Specific GHG-Emissions per year ($kg_{CO_{2,eq}}$/N•year)
T	Thrust force (N)
$TSFC$	Thrust specific fuel consumption (g/Nh)
u	Stream velocity (m/s)
η	Engine global energy efficiency (% J/J)
ν	Kinematic viscosity of the fuel blend (m^2/s)
Subscript	**Definition**
0	Intake air
C	Carbon
a	Air
ad	As determined basis
e	Exhaust gas
f	Fuel
$norm$	Normalized value for optimum trade-off
st	Stoichiometric

Biodiesel is the preferred biofuel to use in a partial substitution mostly in terms of its chemical compatibility, considering that aviation Jet Fuels are mainly an intermediate distillate from petroleum, and due to its high worldwide availability [10]. Biodiesel has been widely studied as an alternative fuel for gas turbine engines, not only for thrust generation in aircraft [11–13] but also, for power generation systems [14–16]. Conventional biodiesel is a mixture of Fatty Acid Methyl Esters – FAME, derived mainly from vegetable oils that have shown advantages of miscibility with fossil fuels, high flash point, and no content of sulfur or aromatic compounds [4]. Former studies of biodiesel blends used in gas turbine engines have shown minor detrimental effects on the engine performance when testing blends of biodiesel FAME from different feedstocks and Jet A1 or JP-8 [13]. Its effects include a raise of the Thrust Specific Fuel Consumption - *TSFC* [11], a higher thermal efficiency [8] and a slight decline in the engine acceleration time [17]. One of the main concerns is linked to the density and viscosity of the biodiesel FAME, which can be 1,2 and 4 times higher than the regulated limits in the aviation fuel standards, respectively. This adversely affects the atomization of fuel by reducing almost 50% of the spray angle when using a mixture of 50% of soybean biodiesel [7].

Furthermore, the effects of the biodiesel viscosity have been appreciable on the exhaust gas emissions of turbine engines operating with biodiesel blends, showing a significant rise in CO emissions related to larger fuel droplets in the atomization and incomplete combustion [12,18]. Nonetheless, Rehman et al. [19], Kimble et al. [20], and Chiaramoniti et al. [13] noted a possible reduction in the evolved CO when increasing the atomization pressure of the biodiesel blend from 0,3 bar to 1,1 bar, leading to better flame stability within the combustion chamber. This reduction also occurred by raising the injection temperature above 120 °C, since the fuel viscosity is reduced when increasing the temperature, thus improving the atomization and volatilization process. A slight reduction in SO_2 was obtained at idle and high-power operating regimes in the same tests [21]. There is no unanimity concerning the NOx and HC emissions of gas turbine engines operating with biodiesel blends. French et al. [17] detected cloudiness of the exhaust stream at low engine power and Corporan et al. [11] reported an increase in the particle emissions near 20% at idle, but a 15% drop at cruise and take-off. The results reported by Nascimento et al. [12] and Habib et al. [8] indicate a lower evolution of NOx and a rise of HC, linked to the higher cetane number and poor atomization of the biodiesel. Lupandin et al. [22], Panchasara et al. [23] and Wang et al. [3] reported a reduction of HC and CO emissions associated with an improved combustion process. Raju et al. [24], studied black carbon emissions when testing a J-85 aviation turbine with blends of catalytic hydro-processed Camelina oil and Jet A1. The authors reported a reduction in the soot particle size when increasing the Camelina oil content due to the lower aromatic concentration. The drawback is related to the dependence of soot formation upon the fuel pyrolysis of Camelia oil.

Some properties of the biodiesel blends do not fulfill the requirements of international aeronautic regulations – such as the current ASTM D1655-19a (for aviation jet fuels) and ASTM D7566-19b (for aviation fuels containing synthesized hydrocarbons as hydro-processed esters and fatty acids – HEFA and biodiesel/FAME) [20]. For instance, the freezing point and waxy particles formation at high altitudes hinder the use of biodiesel in aircraft engines, since the cloud point of biodiesel ranges from −25 °C to 26 °C, which is far from the −40 °C temperature limit given in the standard [18]. Waxy particles formation can be corrected by the mixture of the jet fuel with a biodiesel content below 20%, or even by implementing a pre-heater within the fuel tanks or the injection systems [25]. Also, rapid oxidation of biodiesel was reported in the literature caused by the high total acid number of this biofuel (typically 4 times the limit of ASTM D1655 standard) and its high reactivity with metals (like brass, bronze, copper, and zinc), which promote fuel gelling, solvent problems, and corrosion of many components of the engine. The chemical incompatibility with the fuel systems also causes a degradation effect on rubber seals and hoses, resulting in a malfunction of the control systems and a more severe maintenance routine [26].

Despite the positive benefits of biodiesel utilization, the previously mentioned challenges remain regarding the aeronautic operational safety. Chiefly associated with the mechanical malfunctions and the need to adjust biodiesel properties to aviation standards. Another issue has to do with the high production costs and the low energy density of biodiesel compared to conventional jet fuels [26]. Unfortunately, technical knowledge arising from experimentation on full-scale aeronautical turbines is expensive and complex, limiting most of the research reported in the literature to small size turbojets [27]. For instance, experimental results performed by Nascimento et al. [12], Chiaramoniti et al. [13], French et al. [17] and Habib et al. [8] are limited to micro-turbines with a power rating below 50 kW. Experimentation using full-size turbines with a power rating above 100 kW is only reported in few studies like the ones by Corporan et al. [11], Lupandin et al. [22], Brem et al [28], and the recent publications of Raju et al. [24] and Talero et al. [29]. In that last study, results of testing of a full-scale turbojet engine J69-T-25A (power rating of 640 kW) using blends of Jet A1 and palm oil biodiesel up to 10% of volume content have been presented by the authors of this article [29]. The results revealed no substantial impacts of biodiesel in the engine operation with that substitution volume. Thereupon, a technical discussion approved testing the gas turbine with up to 50% of biodiesel content in the fuel blend, argued by on-field measurements of the Exhaust Gas Temperature - EGT, Thrust, and Mechanical Wearing of the engine parts. The experimental results of the higher-biodiesel content operation are published in the present article, being obtained using parallels in the experimental bench and methodology (safety procedures, mixing facility, and measurement systems) with those former publications [29,30].

Extended analyses are motivated by the lack of experimental information and validation in real aeronautic turbines operating with a relevant content of biodiesel in the fuel blend, including the major absence of information regarding the effects on the energy performance, emissions, and the mechanical wearing of components. Therefore, the main purpose of the current study is to analyze the experimental results of testing a full-scale turbojet engine J69-T-25A with a power rating of 640 kW, operated at a mean sea level of 2554 m using blends of Jet A1 with palm oil biodiesel volume contents. The focus of the present article is on the thermal, mechanical, and economic feasibility analysis of achieving a 50% biodiesel substitution in aircraft turbojet engines without any mechanical adjustments. The inclusion of experimental methods such as the fuel characterization, atomization analysis in the fuel nozzle injectors, and thrust force and exhaust gas measurements expands the technical knowledge necessary to make the biodiesel substitution for commercial aviation feasible. An optimum trade-off between the economic and environmental impacts against the technical drawbacks of this technology is researched in the full-size aviation turbojet engine, which has been traditionally devoted to commercial aircrafts. Special attention has been paid to thermal efficiency at all engine operation regimes and the interaction between the fuel blend and the auxiliary systems of the aircraft. The main findings are related to the overall engine performance and the exhaust emissions by measuring the Thrust force – T, fuel mass flow – $\dot{m}_f$ and volume fractions of O_2, CO_2, CO and HC; and by calculating the Thrust Specific Fuel Consumption – $TSFC$, engine global efficiency – η, Air/Fuel Ratio – AFR and percent Excess combustion Air – $\%EA$.

The remainder of this article is organized as follows. In the Materials and methods section, the methodology and experimental facility of the gas turbine engine are described. Simultaneously, the experimental planning and data processing are explained in that same section. The measured results of different operation scenarios are presented in the Results and discussion section, involving the engine operation with blends of biodiesel and power loads. The discussion about the influence of the biodiesel content in the engine performance, evolved emissions, and the environmental and economic impacts is addressed in that section too, determining some outstanding findings of the deterioration of the engine hot section. Finally, in the last section some conclusions close the article.

Materials and methods

Fuels characterization

Two fuels are used in the present study: a commercial kerosene-based Jet A1 and a Colombian palm oil biodiesel with a commercial reference BioD – Premium 360. The experimental plan on the J69 engine is conducted with fuel blends of Jet A1 and biodiesel using the following Biodiesel Volume Contents - w_{BD}: 0% (B0), 10% (B10), 20% (B20), 30% (B30), and 50% (B50). The blends are prepared in a tank trailer (nominal capacity of 4 m^3), using a transfer pump and a flow meter Tuthill Fill-Rite model 820 (accuracy of 0,1%). An initial volume $V_{i,B0} = 1762 \pm 8$ L of Jet A1 is filled in the tank trailer and consumed in the baseline experiments B0 until a final volume $V_{f,B0}$ is obtained. Thereafter, a volume of biodiesel is added to the tank trailer to increase the biodiesel volume fraction to 10%. The new volume $V_{i,B10}$ is used in the experimental levels B10 until a final volume $V_{f,B10}$ is accomplished. This procedure is repeated for the experimental levels B20, B30, and B50, successively. The accuracy of the volume contents of biodiesel is always kept below 2,5%.

The characterization of the Jet A1, the palm oil biodiesel, and the fuel blends are presented in Table 1, including a compilation of

Table 1
Characterization of biodiesel and Jet A1 fuels used in this study. Measured and gathered values from the literature [11,13,14,21,31], including the aviation fuel standards: ASTM D1655-19a (for fossil fuels), ASTM D7566-19b (for fuels containing synthesized hydrocarbons), and DIN EN 14,214 (for FAME).

Properties	Unit	Current study						Literature		Aviation fuels standard		
		B0 Jet A1	B10	B20	B30	B50	B100 biodiesel	JetA1	Biodiesel	ASTM D1655	ASTM D7566	DIN EN 14,214
Density 15 °C	kg/m^3	809,5 ± 1,8	823,2	827,1	832,3	835,1	841,1 ± 3	807	881	775–840	730–772	860–900
νat 40 °C	mm^2/s	1,42 ± 0,01	1,61	1,76	1,99	2,52	4,53 ± 0,11	1,2	3,7	1,9–6,0	< 8,0	3,5–5,0
Pour point	°C	3	n.m.	n.m.	n.m.	n.m.	12	−45	−12	n.r.	n.r.	n.r.
Flash point	°C	60	n.m.	n.m.	n.m.	n.m.	181	39,5	173	> 38	> 38	> 101
Cloud point	°C	n.d.	n.m.	n.m.	n.m.	n.m.	14	−53,4	−19	< −47	< −40	n.r.
Cetane number	–	> 45	n.m.	n.m.	n.m.	n.m.	58	46	53	n.r.	n.r.	> 51
Acid value	mg$_{KOH}$/g	n.d.	n.m.	n.m.	n.m.	n.m.	0,323	n.r.	n.r.	< 0,1	< 0,015	< 0,5
HHV_{ad}	MJ/kg	45,41 ± 0,07	44,8*	44,3*	43,7*	42,6	39,70 ± 0,02	42,9	39,9	> 42,8	> 42,8	n.r.
AFR_{st}	g$_{air}$/g$_{fuel}$	21,64	20,98	20,34	19,72	18,55	15,98	n.r.	n.r.	n.r.	n.r.	n.r.
C_{ad}	% g/g$_{fuel}$	82,79 ± 1,57	82,2*	81,6*	80,9*	79,7*	76,74 ± 0,51	86,4	77,3	n.r.	n.r.	n.r.
H_{ad}	% g/g$_{fuel}$	13,01 ± 0,23	12,9*	12,9*	12,8*	12,7*	12,38 ± 0,03	13,6	12,1	n.r.	n.r.	n.r.
N_{ad}	% g/g$_{fuel}$	1,26 ± 0,08	1,24*	1,21*	1,19*	1,14*	1,02 ± 0,18	n.r.	n.r.	n.r.	n.r.	n.r.
O_{ad}**	% g/g$_{fuel}$	1,90 ± 0,51	2,70	3,49	4,29	5,88	9,86 ± 0,72	n.r.	10,6	n.r.	n.r.	n.r.
S_{ad}	mg/kg$_{fuel}$	< 350	n.m.	n.m.	n.m.	n.m.	1,1 ± 0,01	50,3	10	< 300	< 15	< 10
Moisture (M_{ad})	mg/kg$_{fuel}$	n.d.	n.m.	n.m.	n.m.	n.m.	102	n.r.	n.r.	< 250	< 75	< 500
Methyl palmitate	% g/g$_{fuel}$	n.d.	3,13*	6,25*	9,38*	15,6*	31,26 ± 1,17	n.d.	42,5	n.r.	n.r.	n.r.
Methyl oleate	% g/g$_{fuel}$	n.d.	4,84*	9,7*	14,5*	24,2*	48,42 ± 1,97	n.d.	41,5	n.r.	n.r.	n.r.
Methyl steate	% g/g$_{fuel}$	n.d.	0,39*	0,78*	1,16*	1,94*	3,88 ± 0,1	n.d.	4,2	n.r.	n.r.	n.r.
n-dodecane	% g/g$_{fuel}$	3,05 ± 0,2	2,75*	2,44*	2,14*	1,53*	n.d.	3,57	n.d.	n.r.	n.r.	n.r.
n-alkanes	% g/g$_{fuel}$	19,67 ± 2,02	17,7*	15,7*	13,8*	9,8*	n.d.	19,35	n.d.	n.r.	n.r.	n.r.

n.d. – Not detected.
n.r. – Not reported.
n.m. – Not experimentally measured.
*Calculated considering a linear response in terms of the biodiesel content and with mass balance of the elements and the CG components.
**Determined by difference.

experimental values reported in the literature [11,13,14,31] and the regulated limits in the aviation fuel standards. The density, kinematic viscosity – ν, pour point, flash point, cloud point, cetane number, and acid value are determined for both biodiesel and Jet A1, according to the ASTM D4052-16, ASTM D445-15, ASTM D97-17b, EN 2719, ASTM D2500, EN 15195, and EN 14104 standards, respectively. The ultimate analysis – CNHO of both fuels is performed according to the EN 15104 standard in a Thermo Scientific Flash 2000 organic elemental analyzer. The sulfur content – S_{ad} is determined according to DIN EN 20884 and the oxygen content – O_{ad} is measured by calculating the mass difference in the products. The moisture content – M_{ad} of both biodiesel and Jet A1 is measured by applying a Karl-Fisher titration according to the ASTM D6304-16 standard.

The Higher Heating Value – HHV_{ad} is determined experimentally for three samples (Jet Fuel, Biodiesel FAME, and 50% volume mixture of the previous two), according to the standard ASTM D240-14 by Bomb Calorimeter. Additionally, chromatographic analysis is carried out to determine the content analysis of hydrocarbons in the Jet Fuel A1 and the FAME in the biodiesel by gas chromatography – GC in an Agilent 6820 equipment. A Flame Ionization Detector – FID, fused silica (0,3 m × 0,53 mm) precolumn and a Supelco SGE HT-5 fused silica capillary column (12 m × 0,53 mm × 0,15 mm) are used. To perform the GC, tricaprine is added as internal standard, and hexane is used as a solvent for preparing samples, manually injecting 1 µL. For hydrocarbons, after 1 min of stabilization at 70 °C, the oven temperature is programmed to increase from 70 °C to 380 °C at 25 °C/min. For FAME, the oven temperature is stabilized at 140 °C for 1 min, then, the temperature increases from 140 °C to 380 °C in 12 min, and it is retained for 5 min. The carrier gas is nitrogen with a flow rate of 4 mL/min and a 50:1 split ratio for hydrocarbon determination, while the flow rate is 6 mL/min for FAME. The flows of H_2 and dry air are 40 mL/min and 360 mL/min, for both hydrocarbons and FAME, respectively.

For the fuel blends (B10, B20, B30, and B50), only properties like density, ν, HHV_{ad}, ultimate composition, and content of hydrocarbons are reported in Table 1, as they are relevant during the ground testing of the turbine. However, the pour point, flash point, cloud point, and the acid value are excluded from the characterization of the fuel blends, as they are pertinent only for flight tests. The density and ν are experimentally determined for all the fuel blends. The HHV_{ad} is experimentally measured only for B50 and is calculated for the remaining blends (B10, B20, and B30) considering a linear interpolation in terms of the biodiesel content. The last approach has a deviation of 0,06% with respect to the measured values of HHV_{ad} (achieved for the B0, B50 and B100), thus they can be estimated without significant error. The ultimate analysis – CHNO and the content of hydrocarbons of all the fuel blends are calculated with a mass balance, considering a linear response in terms of the biodiesel content. Indeed, the GC and the CHNO characterization are not mandatory for all fuel blends since the hydrocarbons of Jet A1 are chemically inert to esters of FAME under standard conditions and no chemical reactions are presented during the preparation of the blends [32,33]. Also, the effects of antioxidants in the biodiesel suggest that fossil fuels have a negligible effect on the mixture stability [34]. Finally, a linear response of the ultimate composition and the content of hydrocarbons against the biofuel content is also reported in the literature [32–36], where a R-squared above 95% concerning experimental data is reported. Hence, the linear estimation can be carried out without significant error.

In general, similar values in the literature have been reported to the ones obtained in the present study [11,13,14,21,31]. Remarkably, the pour point significantly differs in both fuels from the values reported in the literature [37]. The GC analysis for Jet A1 (B0) shows that about 37% corresponds to linear hydrocarbons, while the rest is composed mainly of branched hydrocarbons and some aromatics. About 3% corresponds to n-dodecane, which is one of the typical components [14]. Due to the high proportion of linear alkanes, the Jet Fuel has both a lower average boiling temperature than that of diesel and a higher-octane number than that of gasoline [38]. The GC analysis for the biodiesel sample (B100) indicates that 84% corresponds to methyl oleate, methyl stearate, and methyl oleate, which are the main FAME components whose values are similar to those reported in literature [32,39,40]. The methyl oleate and methyl palmitate are found in a greater proportion, and the composition of these three methyl esters

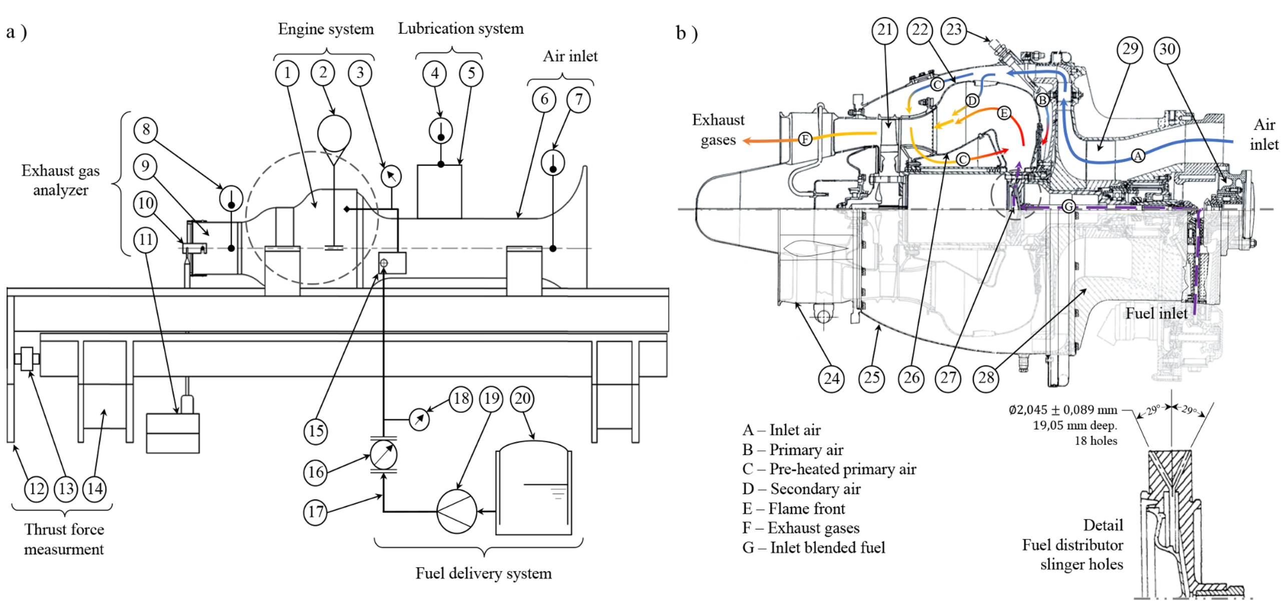

Fig. 1. (a) General J69 engine experimental facility detailing peripheral components and instrumentation: (1) turbojet engine model J69T-25A, (2) tachometer, (3) fuel pressure manometer, (4) oil supply temperature thermocouple, (5) oil supply tank, (6) air inlet duct, (7) air inlet temperature probe set, (8) EGT thermocouple set, (9) outer tailpipe, (10) exhaust gas sampling rake, (11) exhaust gas analyzer, (12) testing platform of horizontal movement, (13) thrust force load cell, (14) fixed testing platform, (15) fuel pump group and fuel control unit, (16) fuel flow meter, (17) fuel supply line, (18) fuel inlet pressure manometer, (19) fuel supply pump, and (20) fuel tank. (b) Detail of the J69 engine including its main components and the steams of air and exhaust gas: (21) turbine rotor, (22) outer combustion shell, (23) starting igniter plug and fuel nozzle, (24) exhaust duct, (25) turbine housing, (26) inner combustion shell, (27) fuel distributor, (28) compressor housing, (29) compressor rotor and (30) starter-generator drive. Source: The Authors.

indicates the palm oil origin of this biodiesel. The presence of oxygen in the fuel blends (corresponding to the ester group of the added FAME biodiesel) is the fundamental cause of the variations in the physico-chemical and functional properties, like the HHV_{ad} reduction [7]. Indeed, when adding FAME biodiesel to the Jet A1, the HHV_{ad} is practically reduced linearly due to the low value of the FAME biodiesel HHV_{ad} (by 12,6%). As a result, the HHV_{ad} is supposed to portray a linear response in terms of the biodiesel content, as experimentally verified in the present study and in [7]. Although the HHV_{ad}, ultimate composition, and the content of hydrocarbons are calculated assuming a linear response in terms of the biodiesel content, the calculated results are not linear as it will be discussed in Section 3.

Experimental facility

Fig. 1 presents the experimental facility employed in the current study. It consists of a ground test bench for the Teledyne CAE – J69 turbojet engine used by the Colombian Air Force in the military aircraft Cessna T-37. The engine is equipped with a dual fuel injection system including slinger holes and fuel nozzles that allows a wide range of fuel operation without breaching the manufacturer specifications. It is used in the present study since its operation using blends of biodiesel has been tested and described in former publications [29], also integrating a more general experimental framework. The engine is installed on a testing bench built following the standard MIL-E-5007D (2) from the Department of Defense of the United States of America and the Teledyne CAE engine manufacturer T.O. 2 J-J69-72 technical manual [41]. Fig. 1a depicts the main components of the experimental facility: the turbojet engine, the control and instrumentation sets, the thrust force measurement system, the fuel delivery system, the exhaust gas temperature measurement, the vibrations control of the compressor and turbine, the exhaust gas sampling stand, and the lubrication system.

The Teledyne CAE – J69 is a single spool turbojet engine of the model variant J69-T-25A with the main technical specifications as indicated in the specific literature of the engine [29,41]. This engine is equipped with a single-stage centrifugal compressor and a single-stage axial turbine that operates at a maximum shaft rotational speed of 21,730 RPM and generates 640 kW and a maximum thrust of 4450 N at ISA conditions. The combustion system is designed to operate with kerosene-based fuels like the Jet A and Jet A-1, and naphtha-type fuels like the JP-4, delivering maximum fuel consumption of 0,143 kg/s. Experimentation is carried out in the operating environment of Madrid, Colombia with a mean sea level of 2554 m, the barometric pressure of 1017 hPa, atmospheric temperature ranging from 16 °C to 26 °C, and relative moisture from 25% to 56%. Considerable differences exist between the engine performance under International Standard Atmosphere (ISA) conditions and at the current study location.

Fig. 1b presents the inner assembly of the J69 engine with the streams of air, exhaust gas, and fuel. The inlet air stream – A is pressurized in the compression housing to a maximum pressure ratio of 3,9 and then propelled into the turbine housing where it is separated into three different flows: the primary airflow – B (5% of total airflow volume); the pre-heated primary airflow – C (70% of total airflow volume); and the secondary airflow – D (25% of total airflow volume). The inlet fuel flow – G is pumped from the Fuel Control Unit – FCU into the starting fuel nozzle only during the start-up procedure of the engine. This flow is mixed with the airstream B to start the combustion, and then pumped into the fuel distributor during steady-state operation. The streams C and D are mixed with the fuel coming from the distributor once the flames reach steady-state conditions. The fuel distributor is a hollowed shaft joined to the turbine main shaft and is responsible for injecting fuel into the combustor chamber through 16 slinger holes. The streams C and D are also used to cool down the combustion chamber. The exhaust gas stream – F expands at the turbine and is cooled down later below 663 °C when it reaches the outer tailpipe.

The instrumentation used in the testing bench is presented in Table 2, which fits with the indications of the engine technical manual - T.O. 2 J-J69-72 [41]. The Outer Air Temperature – OAT and Exhaust Gas Temperatures – EGT are measured with a set of 6 thermocouples installed at the air inlet duct and at the outer tailpipe, respectively. An exhaust gas sampling rake is installed at the outer tailpipe with a design that meets the standards of the International Civil Aviation Organization [42] and according to the experimental facility proposed by Talero et al. [29]. The fuel blends stored in the tank trailer is then pumped with an external transfer pump (345 kPa of max. pressure and flow ranging from 20 L/min to 120 L/min) into the Fuel Control Unit – FCU. The FCU is a hydro-mechanical component that controls the dosing of fuel by modifying the opening of a set of needles valves as a function of the ω_{shaft}, EGT, acceleration control, and the sensed pressure of the pre-heated primary air. Note that no mechanical adjustments of the engine or the inclusion of external components to assure its functionality are involved in the experiments.

Experimental planning and procedure

In order to evaluate the effect of the biodiesel substitution in the engine performance a full factorial experimental design is build [43,44]. For the independent parameters, a set of 5 levels of biodiesel contents – w_{BD} described in the previous section together with 4 levels of engine load (in terms of a percentage ratio of the maximum ω_{shaft} of 21,730 RPM) are tested and codified with the acronym "B" and "RPM", respectively. The engine regimes are selected to evaluate the most frequently operating power loads during a flight, as follows. The Idle – 38% RPM (8257 ± 165 RPM) regime is selected to test the stabilization condition after the start-up of the engine with no acceleration. The Cruise – 80% RPM (17384 ± 347 RPM) and 70% RPM (15211 ± 305 RPM) regimes are used to evaluate the performance of the engine at

Table 2
Instrumentation used in the testing bench of the J69 engine fitting the indications of the engine technical manual - T.O. 2 J-J69-72 [41] and according to the experimental facility proposed by Talero et al. [29].

Variable	Instrument	Range	Accuracy
Fuel mass flow $-\dot{m}_f$	Flow meter Tuthill Fill-Rite model 820	7,6 L/min to 75,7 L/min	± 0,5%
Rotational speed of the main shaft $-\omega_{shaft}$	Tachometer generator ref. AAE and model MS25038-4	0 RPM – 4200 RPM, speed ratio of 6:1	± 1%
Thrust force $-T$	2 load cells Toroid model Corp. 3965	0 kg–11,340 kg	± 1%
Volume fractions at te exhaust gas of O_2, CO_2, CO, HC	Gas analyzer Hanatech ref. IM2400 Ultra 4/5	0–23%, 0–20%, 0–10% and 0–10,000 ppm for the O_2, CO_2, CO, and HC, respectively	± 1%
Exhaust Gas Temperature – EGT	6 thermocouples Ref. 700, 530	−270 °C to 1260 °C	± 1%
Air Inlet Temperature – OAT	6 thermocouples Ref. 700, 530	−270 °C to 1260 °C	± 1%
Temperature of ambient air	Thermo-hygrometer Omet ref. C3121	−30 °C to 105 °C	± 0,4 °C
Relative humidity of ambient air	Thermo-hygrometer Omet ref. C3121	0% to 100% RH	± 2,5% RH
Barometric pressure	Barometer Wallace and Tiernan ref. FA 112, 170	64 kPa to 108 kPa	± 0,1%

minimum thrust during the taxing of the aircraft. Finally, the Take-off–100% RPM (21730 ± 435 RPM) regime normally reports the maximum power generation and fuel consumption used during the take-off and landing of the aircraft. These regimes are initially tested using pure Jet A1 (experiments B0-RPM38, B0-RPM70, B0-RPM80, B0-RPM100) and are selected as the baseline experiments. The biodiesel volume contents (B10, B20, B30, and B50) are chosen to gradually study the effect of biodiesel substitution in the engine operation and to facilitate comparability with results in the literature. The main response variables of the experimental design are the air to fuel ratio, percent excess combustion air, thrust specific fuel consumption, and engine global efficiency.

One typical experimental run is performed according to the "maintenance testing procedures" of the manufacturer reported in the T.O. 2 J-J69-72 technical manual [41], with minor variations reported in [29] that facilitate biodiesel fuel blends tests. After the start-up procedure, the engine is gradually speeded up to Take-off until the temperature of the lubrication oil reaches steady-state conditions. After 5 min in a steady-state, the response variables are registered. The variables OAT, EGT, ω_{shaft}, T, and P_f are measured and collected every 5 s only during the steady-state conditions and using a National Instruments ref. cRIO data logger. The value of $\dot{m}_f$ and the volume fractions of O_2, CO_2, CO, and HC at the exhaust gas are manually registered every 15 s only during the steady-state conditions. This registration procedure is repeated for the Idle, intermediate 70% RPM, and Cruise regimes. Upon Idle, an acceleration test is done three times by measuring the response time – t_{ac} of the engine from 8257 RPM until reaching 21,730 RPM. Finally, to identify the contamination of the main components of the engine, a visual inspection is done before and after each experimental run.

To perform the uncertainty analysis of the experimental measurements, three test replicas are done for each tested engine regime and fuel blend, driving a total number of 80 experiments. In addition to the 3 replicas officially reported, a total number of 10 preliminary replicas were performed for the baseline experiment with pure Jet A1 fuel. As a remark, the measured variables are acquired 20 times for each replica during steady-state conditions and all the instruments presented in Table 2 are calibrated before the experimental runs, according to the standard MIL-E-5007D (2). The last approach provides enough data to have the significance of the statistics and to perform an ANOVA test including two-factor interactions. The uncertainty of the measured variables is reported in Table 4 and the max. coefficients of variations are obtained as follows: T is 4,2%, EGT is 0,4%, $\dot{m}_f$ is 2,3%, and P_f is 2,5%. These statistical results allow concluding a 95% confidence for the uncertain estimates of the experimental tests. Significant variations of $TSFC$ and η against w_{BD} are reported by the ANOVA test at Idle regime, but no statistically significant difference is observed at Cruise and Take-off regimes for the different biodiesel contents.

Data processing and thermal calculations

To evaluate the performance of the engine, post-process calculations are performed with the acquired data. $TSFC$ and η are the main variables to be analyzed. $TSFC$ is calculated with Eq. (1). In contrast to the η or AFR, this variable has a low uncertainty since it only depends over the experimentally measured quantities fuel mass flow – $\dot{m}_f$ and thrust force – T.

$$TSFC = \frac{\dot{m}_f}{T} \quad (1)$$

In the case of the global efficiency – η, it must be computed with the post-processed thermal quantities of the engine, like air mass flow – $\dot{m}_a$, exhaust gas mass flow – $\dot{m}_e$, and AFR. Thus, the mass balance of the gases flowing through the engine must be first addressed. Since $\dot{m}_f$ is a measured quantity, $\dot{m}_a$ can be computed from Eq. (2). The $\dot{m}_e$ includes both the $\dot{m}_a$ and the burnt fuel at the combustion chamber $\dot{m}_f$, hence it can be computed with Eq. (3).

$$\dot{m}_a = \dot{m}_f AFR \quad (2)$$

$$\dot{m}_e = \dot{m}_a + \dot{m}_f = \dot{m}_f(1 + AFR) \quad (3)$$

To determine the AFR, a global combustion reaction is assumed according to Eq. (4), using the methodology proposed by Ali et al. [31]. In that reaction, the mass of the fuel – m_f and the air of combustion – m_a are calculated according to Eq. (5) by using the experimentally measured volume fractions of CO and CO_2 in the exhaust gas analysis and the ultimate composition of the fuel blend (reported in Table 1) of each experiment. The estimation of AFR can be carried out without significant error even assuming a linear response to calculate CHNSO, due to the strong linear correlation reported in literature respect to experimental data and to the chemical background of non-reactivity of biodiesel and Jet A1 in the blends [32–36]. Note that the stoichiometric Air to Fuel Ratio – AFR_{st} depends only on the ultimate composition of each fuel blend, in terms of the atomic ratios x, y and z of Eq. (4). The AFR_{st} for each fuel blend is reported in Table 1, assuming a stoichiometric combustion (in Eq. (4) $c = d = 0$ and neglecting the air moisture content), then, finding a molar stoichiometric air to fuel ratio of $a/f_{st} = (x + y/4 - z/2)/0,25$. Finally, the $\%EA$ is calculated with Eq. (6) and relates at the same time the measured variations of m_f and m_a with the theoretical complete combustion of the fuel blend, allowing a wider analysis of the combustion.

$$fC_xH_yO_z + a(0,77N_2 + 0,25O_2 + 0,019H_2O) \rightarrow bC O_2 + cCO + dO_2 + eN_2 + gH_2O \quad (4)$$

$$AFR = \frac{m_a}{m_f} = \frac{a}{f}\frac{MW_a}{MW_f} = \frac{w_{C,f}MW_a/MW_C}{X_{CO_2} + X_{CO}} \quad (5)$$

$$\%EA = \frac{AFR}{AFR_{st}} - 1 \quad (6)$$

The air intake velocity – u_0 is calculated using Eq. (7), where the ambient air density ρ_0 is determined as an ideal gas mixture with its properties evaluated at the operating environmental conditions, and the cross-sectional area being $A_t = 9,079\ m^2$. To calculate the exhaust gas velocity – u_e, a momentum balance of the engine installed in the testing bench is formulated according to Eq. (8). It is assumed that the pressure of the exhaust gas is approximately the intake air pressure and that the thrust force is equal to the momentum difference between the intake air and the exhaust gas.

$$u_0 = \frac{\dot{m}_a}{\rho_0 A_t} \quad (7)$$

$$u_e = \frac{T + \dot{m}_a u_0}{\dot{m}_e} \quad (8)$$

The engine global efficiency is defined as the ratio of the power produced by the engine to the power supplied by the fuel. The global efficiency – η is calculated with Eq. (9) according to Ali et al. [31] and Z. Habib et al. [8], where the power produced by the engine is composed of the generated thrust power and the rate of kinetic energy delivered to the airstream.

$$\eta = \frac{Tu_0 + \frac{1}{2}\dot{m}_a\left(1 + \frac{1}{AFR}\right)(u_e - u_0)^2}{\dot{m}_f HHV_f} \quad (9)$$

To complement the thermal calculation with the statistical analysis of the results, an optimum trade-off analysis of the biodiesel in the blend, based on the measured results, is addressed in the present work using the methodology proposed by Talero et al. [45]. This analysis aims to avoid a significant reduction of η, a relevant increase in t_{ac} and the raise of $\%EA$ (as an indicator of the combustion efficiency), when increasing the biodiesel content in the fuel blend. Normalization of the global energy efficiency – η_{norm}, acceleration time – $t_{ac,norm}$, and combustion percent Excess Air – $\%EA_{norm}$ are calculated using Eqs. (10) to Eq. (12).

$$\eta_{norm} = \frac{(\eta_{B0} - \eta)}{(\eta_{B0} - \eta_{50})} \quad (10)$$

$$t_{ac,norm} = \frac{(t_{ac,B50} - t_{ac})}{(t_{ac,B50} - t_{ac,B0})} \quad (11)$$

$$\%EA_{norm} = \frac{(\%EA_{B50} - \%EA)}{(\%EA_{B50} - \%EA_{B0})} \quad (12)$$

The trade-off analysis is performed using the results at Idle since it demonstrates the greatest performance variations. Continuous functions for each variable over the blend compositions are constructed using a third-order-polynomial regression. The trade-off blend composition can be addressed thereby by locating the intersection point of those three profiles.

Finally, to evaluate the economic and environmental impact of the substation of biodiesel on the J-69 engine operation, the Specific Operating Cost per year – SOC and the Specific GHG-Emissions per year – SGE are calculated per unit of thrust force – T, according to Eqs. (13) and (14), respectively.

$$SOC = 8760(Cost_{fuel}/kg)_{fuelblend}TSFC \quad (13)$$

$$SGE = 8760(kg_{CO_{2,eq}}/kg)_{fuelblend}TSFC \quad (14)$$

These indicators are calculated in order to involve the detrimental of the engine's performance in terms of the $TSFC$. For the SOC, only the fuel consumption is considered as a variant cost with a linear response in terms of the biodiesel content, assuming average 2019 fuel prices for Jet A1 and biodiesel B100 of 5,50 USD/kg_f and 11,48 USD/kg_f, respectively (values reported by U.S. Department of Energy [46]). In the case of the SGE, the GHG-emissions are supposed to be linear in terms of the biodiesel content, assuming $CO_{2,eq}$ releases for the Jet A1 and biodiesel B100 of 85 $kg_{CO_{2,eq}}/GJ$ and 40 $kg_{CO_{2,eq}}/GJ$, respectively (values reported by Wang et al. [47]). In both SOC and SGE, the $TSFC$ is chosen to be the Cruise value, as it is the longest-lasting operative regime of the engine.

Results and discussion

Table 3 compiles the measured results that have been obtained in the tests following the experimental plan. The experimental measurements of the engine performance are detailed for all the operation regimes and the B0, B10, B20, B30, and B50 biodiesel blends. The results presented in that table aim to quantify the effect of the biodiesel on the engine operation variables, but also on the evolved emissions during the combustion process. Likewise, Figs. 2 and 3 show the results of the AFR, $\%EA$, $TSFC$, and the calculated variables for the different blends and operation regimes.

Analysis of the baseline experiments

As baseline experiments, the engine responses to operation with the Jet A1 (B0) at Idle – B0-RPM38, B0-RPM70, Cruise – B0-RPM80, and Take-off – B0-RPM100 are first described. It can be noticed that the minimum and maximum values of T, $\dot{m}_f$ and P_f are attained at Idle and Cruise, respectively. The minimum EGT value occurs between the 70% RPM and the 80% RPM Cruise regimes, as a result of the optimal heat dissipation of the engine [41]. The values of AFR, $TSFC$, and η are similar to those reported in the literature for turbojet aviation engines [18,21], ranging above 50 in the case of the AFR and below 15% for the η.

Furthermore, it can be observed from Fig. 2 that the minimum AFR values occur during Take-off and Idle regimes. The maximum EGT occurs at those same regimes due to the poor heat dissipation of the engine. This is explained by the low transferred heat to the air stream compared to the released heat during the combustion. The low AFR at Idle also determines an increased CO and HC production. Nonetheless, a detailed study of the CO and HC shows a production drop at higher speeds, with a minimum between Cruise and Take-off regimes.

A remarkable finding is related to the calculated exhaust gas velocity – u_e which increases proportionally to the ω_{shaft}. The calculated Mach Number – Ma of the exhaust gas varies from 0,25 to 0,72 at Idle and Take-off regimes, respectively. Therefore, it can be observed that the maximum rate of kinetic energy delivered to the airstream is around 98,3 ± 0,9% of the total engine power. Oppositely, the thrust power represents only 1,7% of the total released power. In the case of the η and $TSFC$ results at the Take-off regime in Fig. 3, those demonstrate maximum and minimum outcomes, respectively.

Table 3
Measured (T, $\dot{m}_f$, EGT, and P_f) variables and exhaust gases composition. The standard deviation of experiments is calculated with three experimental replicas.

Operating regimes	Experiment	Measured variables					Exhaust gases*				
		w_{BD} %	T N	$\dot{m}_f$ g/s	EGT °C	P_{fuel} kPa	O_2 %	CO_2 %	CO %	HC ppm	u_e m/s
Base line experiments	B0-RPM38	0	283 ± 12	24,7 ± 1,1	557 ± 2,4	641	17,0	2,97	0,40	22,4	168 ± 28
	B0-RPM70	0	956 ± 40	42,5 ± 1	467 ± 2	968	17,5	2,66	0,11	3,3	283 ± 35
	B0-RPM80	0	1355 ± 56	53,8 ± 1,3	473 ± 2	1081	17,6	2,63	0,08	0,8	318 ± 23
	B0-RPM100	0	2676 ± 112	95,6 ± 2,2	590 ± 2,6	1388	16,8	3,39	0,07	0,3	455 ± 7
Idle 38% RPM	B10-RPM38	10	278 ± 12	29,2 ± 0,7	542 ± 2,3	675	17	2,93	0,36	19	151 ± 15
	B20-RPM38	20	266 ± 12	29,6 ± 0,7	540 ± 2,3	696	17,1	2,92	0,35	9,6	153 ± 4
	B30-RPM38	30	208 ± 9	30,1 ± 0,7	551 ± 2,4	702	17,1	3	0,34	6,6	110 ± 32
	B50-RPM38	50	196 ± 8	30,8 ± 0,7	539 ± 2,3	715	17,3	2,94	0,31	5,4	115 ± 37
70% RPM	B10-RPM70	10	937 ± 39	46,3 ± 1,1	460 ± 2	992	17,7	2,61	0,11	2,8	257 ± 40
	B20-RPM70	20	921 ± 40	47,9 ± 1,1	458 ± 2	992	17,7	2,59	0,1	0,4	256 ± 31
	B30-RPM70	30	845 ± 35	49 ± 1,1	467 ± 2	980	17,7	2,63	0,1	0	227 ± 11
	B50-RPM70	50	883 ± 37	51,1 ± 1,2	461 ± 2	997	17,9	2,63	0,1	0	237 ± 34
Cruise 80% RPM	B10-RPM80	10	1346 ± 56	57,5 ± 1,3	462 ± 2	1118	17,8	2,63	0,08	0,1	295 ± 12
	B20-RPM80	20	1335 ± 58	58 ± 1,3	461 ± 2	1121	17,7	2,6	0,07	0	306 ± 12
	B30-RPM80	30	1259 ± 52	60,1 ± 1,4	471 ± 2	1105	17,7	2,71	0,07	0	281 ± 9
	B50-RPM80	50	1294 ± 54	61,3 ± 1,4	457 ± 2	1162	17,8	2,69	0,07	0	290 ± 6
Take-off 100% RPM	B10-RPM100	10	2652 ± 113	95,7 ± 2,2	585 ± 2,5	1429	16,9	3,35	0,06	0	455 ± 25
	B20-RPM100	20	2622 ± 114	100,6 ± 2,3	586 ± 2,5	1428	16,8	3,42	0,07	0	451 ± 10
	B30-RPM100	30	2568 ± 107	102,8 ± 2,3	590 ± 2,5	1409	16,8	3,45	0,07	0	421 ± 7
	B50-RPM100	50	2656 ± 110	106,1 ± 2,4	582 ± 2,5	1472	16,9	3,54	0,07	0	442 ± 8

* The max standard deviation for the volume fraction of exhaust gases is as follows: O_2 is 0,13%, CO_2 is 0,04%, CO is 0,04% and HC is 2,5 ppm.

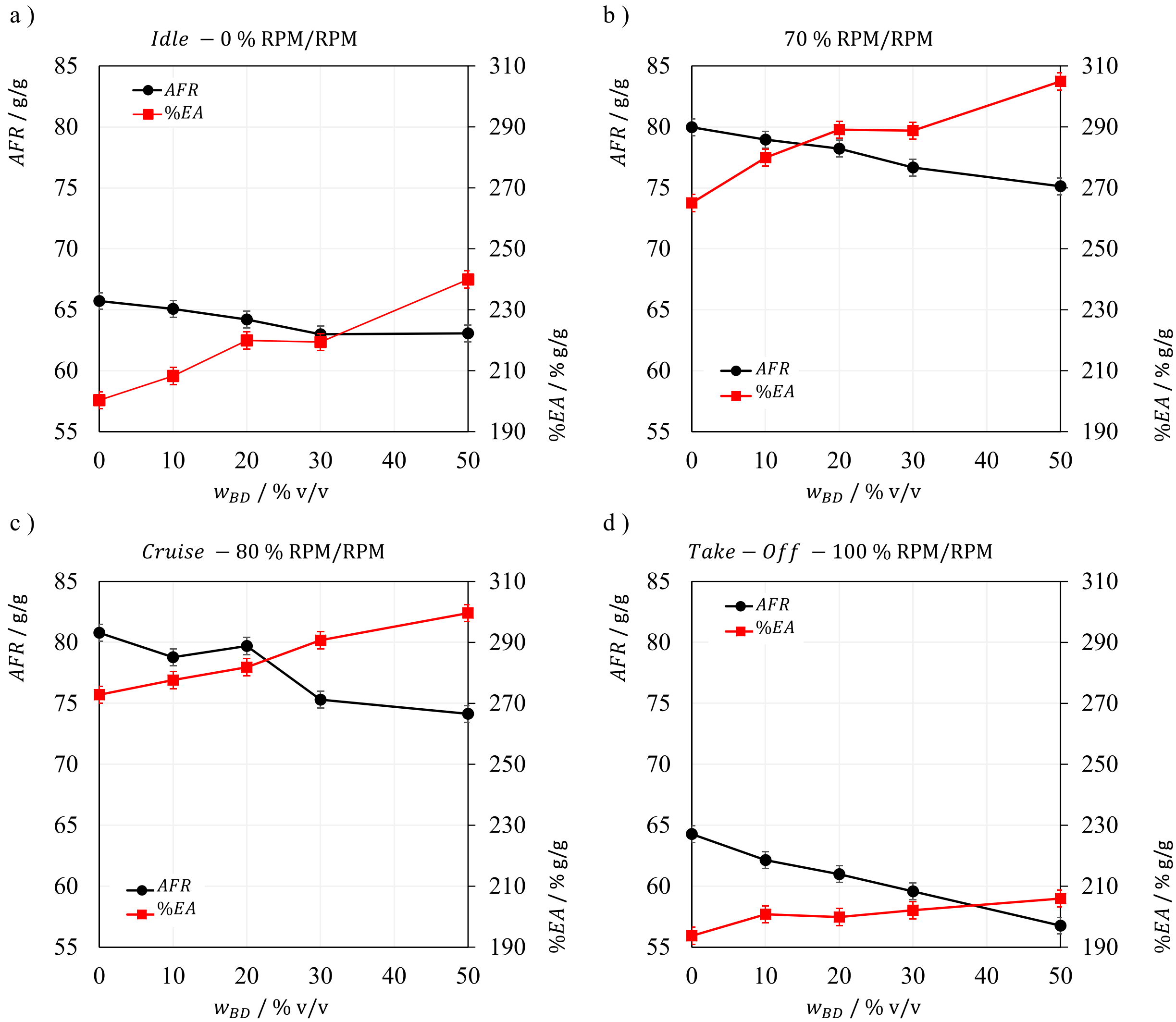

Fig. 2. Results of Air/Fuel Ratio – *AFR* and percent Excess combustion Air – *%EA* for the biodiesel fuel blends at different operating regimes: (a) Idle – 38% RPM (8257 RPM), (b) 70% RPM (15211 RPM), (c) Cruise – 80% RPM (17384 RPM), and (d) Take-off – 100% RPM (21730 RPM).

Influence of the biodiesel on the engine performance and emissions

Next, the engine operation including biodiesel in the fuel is studied. From the results in Table 3, several findings regarding the influence of the biodiesel in the engine performance and emissions can be observed. One first disclosure that has also been reported by Corporan et al. [11] is the 26,6% loss in T and 10,8% increase in $\dot{m}_f$ when adding 50% of biodiesel at Idle. This behavior can be explained by the HHV_{ad} and atomization quality loss given by the fuel blend in contrast to the Jet A1 operation. Note that the HHV_{ad} variation from 45,41 MJ/kg in the B0 to 42,55 MJ/kg in the B50 blend reduces by 3,82% the rate of energy supplied by the fuel.

Another consequence of the biodiesel presence is the raise of *TSFC* and reduction of η at all load regimes. In the case of the B50 operation at Idle regime, the reported *TSFC* is 2,3 times the B0 baseline measure. Indeed, important efficiency η variations are obtained at low load regimes, reinforcing the preponderant influence of biodiesel on the engine operation at these regimes. The opposite is observed at high load regimes, for which the thrust force and the *TSFC* diminish notably (with as much as 3,3% and 6,5%, respectively, at Take-off regime). Habib et al. [8] reported the same *TSFC* reduction tendency when using Jet A1 fuel blends with canola, soybean, and rapeseed biodiesel up to 50% content. Although the findings in the present study expose a reduction in η and a rise in *TSFC*, according to the 95% confidence interval given by the ANOVA analysis, no statistically significant differences are obtained for η and *TSFC* against w_{BD} at Cruise and Take-off regimes. Thus, no significant variations of the energy performance are found in the J69 engine operation with fuel blends at high load operating regimes, denoting a negligible influence of the biodiesel when it is injected to the combustor. This finding indicates a small impact of the biodiesel on the combustion system, but also on the overall performance of the engine at high operation loads.

In that sense, the influence of the dynamic injection of the fuel blend into the combustor is detailed in the present study. The response time to quick throttle variations is a fundamental operating parameter to be considered, as long as the J69 engine is mostly used in military aircrafts. Thus, an increase above 2 s is not recommended by the engine manufacturer [41]. Fig. 4a presents the response time t_{ac} of the engine to reach 21,730 RPM from 8257 RPM for the different biodiesel contents in the fuel blend. A maximum 20% rise in t_{ac} is observed for the B50 fuel blend operation. This behavior has been also reported by French et al. [17], who indicated a 15% increase in the acceleration time for operations with blends of waste oil biodiesel. The findings in that work were explained as the effects of the higher viscosity, droplet formation, and ease of ignition *in-situ* of the fuel blend. Nonetheless, this variation can also be caused by a delay in the FCU response time due to the increase in the viscosity of the fuel blend.

Some detailed and complimentarily experiments are executed to

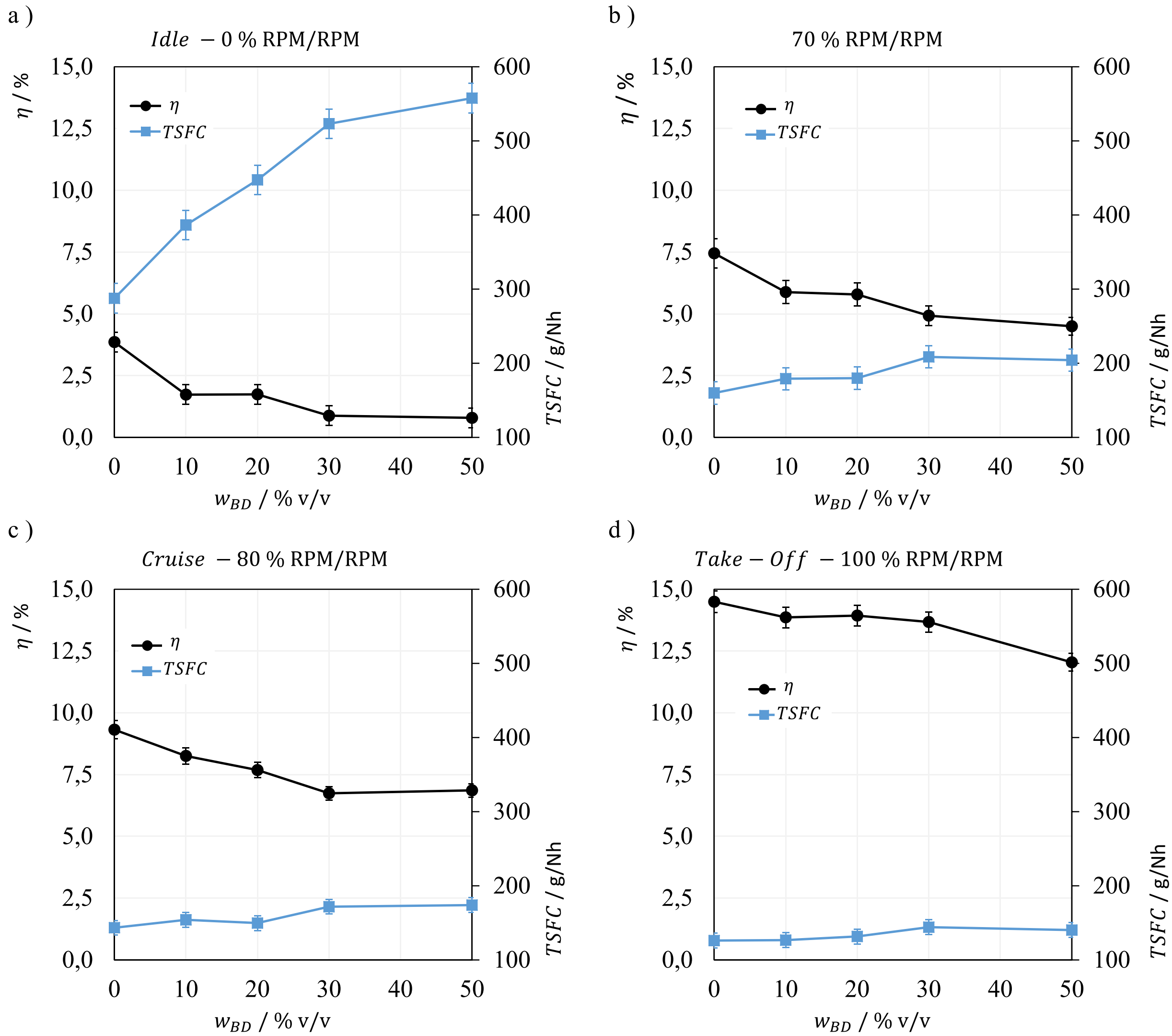

Fig. 3. Results of Thrust specific fuel consumption – *TSFC* and engine global efficiency – *η* for the biodiesel fuel blends at different operating regimes: (a) Idle – 38% RPM (8257 RPM), (b) 70% RPM (15211 RPM), (c) Cruise – 80% RPM (17384 RPM), and (d) Take-off – 100% RPM (21730 RPM).

study the effect of the fuel blend in the acceleration time: the viscosity and atomization angle – θ_{atom} experimental tests are achieved for each biodiesel blend. The atomization angle of the B0, B20, B30, and B50 fuel blends is tested three times with a set of staring fuel nozzles ref. 3034342, by fixing the fuel pressure and temperature to 345 ± 14 kPa and 15 ± 5 °C, respectively. The θ_{atom} is measured by optical inspection and verifying the formation of skewness, drooling, or spitting. The ν of the fuel blend is measured according to the ASTM D 445–15 standard. The experimental results of the θ_{atom} and ν against w_{BD} are presented in Fig. 4b, highlighting a reduction of the atomization angle from 101 ° to

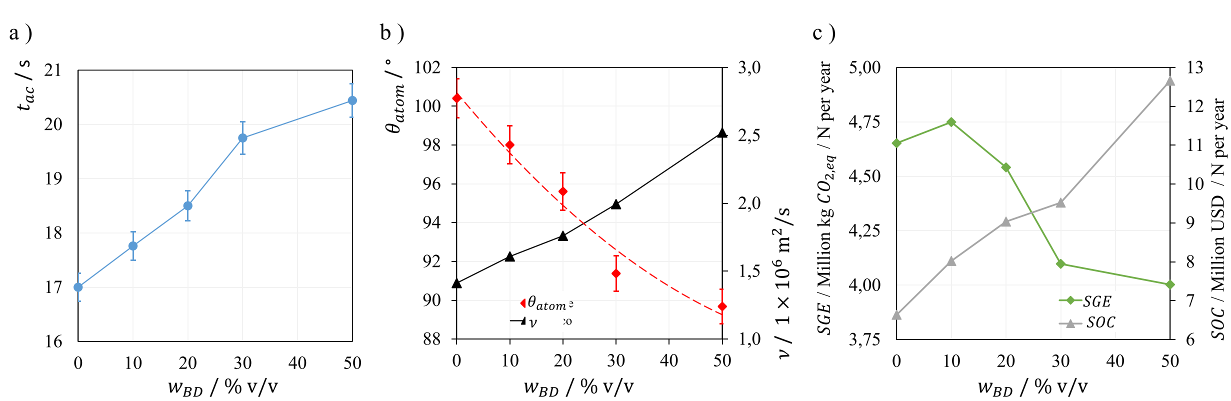

Fig. 4. Biodiesel effects on the gas turbine engine operation. Experimental results concerning: (a) acceleration time t_{ac} from 8257 RPM to 21,730 RPM, (b) atomization angle – θ_{atom} of the fuel nozzle spray and kinematic viscosity – ν of the fuel blend, and (c) Specific GHG-Emissions per year – *SGE* and Specific Operating Cost per year – *SOC*.

89 ° when increasing w_{BD} from 0% to 50%. Although the atomization cones demonstrate a uniform spray quality, some streaks are observed in fuel blends with biodiesel concentration above B20. Nonetheless, no droplet formation for high biodiesel contents is registered in the present study.

The variation in the atomization angle is caused by the viscosity and density increase of the fuel blend [38]. In the case of the B50 mixture, the density only increases around 3,2%, but the viscosity portrays a significant rise of 78,5%. If the blend viscosity is very low during the fuel injection, atomization fluctuations will occur, causing a noisy and unstable combustion flame. On the contrary, the very high viscosity of the blend will cause inadequate atomization. This occurs due to the formation of very large particles that are difficult to vaporize, thus producing incomplete combustion and increasing the soot formation [48]. A more laminar atomization tendency and the subsequent increase in the fuel injection pressure (exposed in Table 3) are observed in the experimental results. These are indicators of either poor atomization [48], fluctuations in the spray drop size [49], or larger droplet concentrations [50] when using high biodiesel contents. Similar behavior has also been reported by Hoxie et al [7], who found a 4,1% drop in the engine kinetic power when including 50% of soybean biodiesel in the traditional fuel. That former finding agrees well with the current η reduction that is depicted in Fig. 3.

The biodiesel effects on the fuel system and burner can be further identified in the combustion exhaust gases [13,20,22,23]. Certainly, a general reduction of the AFR when increasing w_{BD} can be noticed from Fig. 2, which is associated with higher fuel consumption. On the contrary, the $\%EA$ decreases for higher biodiesel contents. This can be explained by the reduction of the AFR_{st} from 21,6 (B0) to 18,5 (B50). It also explains the CO and HC emissions reduction for high biodiesel contents (as registered in Table 3), which can be related to the increased carbon and oxygen ratio of biodiesel [43]. The same conclusion has been reported in the literature: that biodiesel plays a major role in flame stability [51,52]. Moreover, the additional excess air presented in Fig. 2 and the slight reduction of the EGT are indicators of the predominant influence of the secondary air stream (D in Fig. 1b) during the fuel blend combustion.

Since η is not only related to the thrust force but also the combustion reaction and its released heat, the incomplete combustion impact on the engine performance has no clear bias. Particularly, the combustion reaction can be studied in detail by taking into account the $\%EA$, emissions, and fuel atomization. The $\%EA$ exposed in Fig. 2 indicate the boost of the available air during the biodiesel fuel blend combustion. This is also the cause of the CO and HC drops. Thus, the $\%EA$ and emissions suggest a *more complete global reaction*: a conclusion which has been also given in the specialized literature and that is related to a higher content of oxygen in the biodiesel [8,12,31]. On the other hand, note that the less atomization behavior of the biodiesel blend that is found in the current experimental test and that is presented in Fig. 4 advocates to an *incomplete combustion reaction*, which conflicts with that conclusion. Unfortunately, there is no overwhelming evidence to conclude complete or incomplete combustion within the J69 engine. Thus, a detailed examination of the combustion efficiency is advised in future studies.

Although the global reaction cannot be disclosed with the present study, the dependence of the combustion parameters on the global efficiency of the engine can be certainly traced. To this effect, a linear regression analysis is carried out herein. As commented before, the experimental results at Idle regime are chosen to be statistically representative. Hence, the η dependence against $\%EA$, θ_{atom} and HHV_{ad} is presented in Fig. 5, including their relative correlation quantified with the R-squared – R^2. A strong correlation is observed between the efficiency and the θ_{atom} and HHV_{ad} variables (R^2 above 90%). This indicates a high influence of both parameters on the η result at the Idle regime. Although $\%EA$ also demonstrates a significant correlation with η, the R^2 result near 80% shows a lower influence compared to θ_{atom} or HHV_{ad}.

Finally, the global efficiency relationship with the global combustion reaction can be explained as follows. Tentatively, the $\%EA$ and CO and HC emissions give the insight of *complete combustion* [43,53]. Nevertheless, the higher viscosity and density of the biodiesel together with the relevant influence of the poor atomization and HHV_{ad} seem to promote *slower combustion* [54]. Indeed, the lower volatility and higher surface tension of the blended fuels along with the fuel decomposition and oxidation of the m-xylene produce a slower evaporation rate and a slowdown of the reaction [55,56]. All these may cause a stagnant process of the reaction released in the combustion chamber. The immediate consequence is the expansion delay of gases abandoning the optimum design zone in the turbine and hence diminishing the engine thrust. As a result, a drop of global efficiency is observed when increasing the biodiesel content in the fuel blend.

Environmental and economic impact at the optimum trade-off of biodiesel substitution

Remarkably, the substitution of biodiesel over 20% v/v has not been recommended before in the literature. This can be explained since a content of biodiesel in the fuel blend > 20% v/v affects negatively the acceleration time t_{ac} out of the manufacturer recommendations. That amount of biodiesel also generates a 22,1% decrease in the thrust force at the Idle regime. In this sense, the optimum substitution content of biodiesel can be further identified with the aid of the trade-off analysis. To search the optimum biodiesel content, the normalized variation of the engine performance at Idle regime in terms of the normalized efficiency, acceleration time, and percentage excess of air is calculated

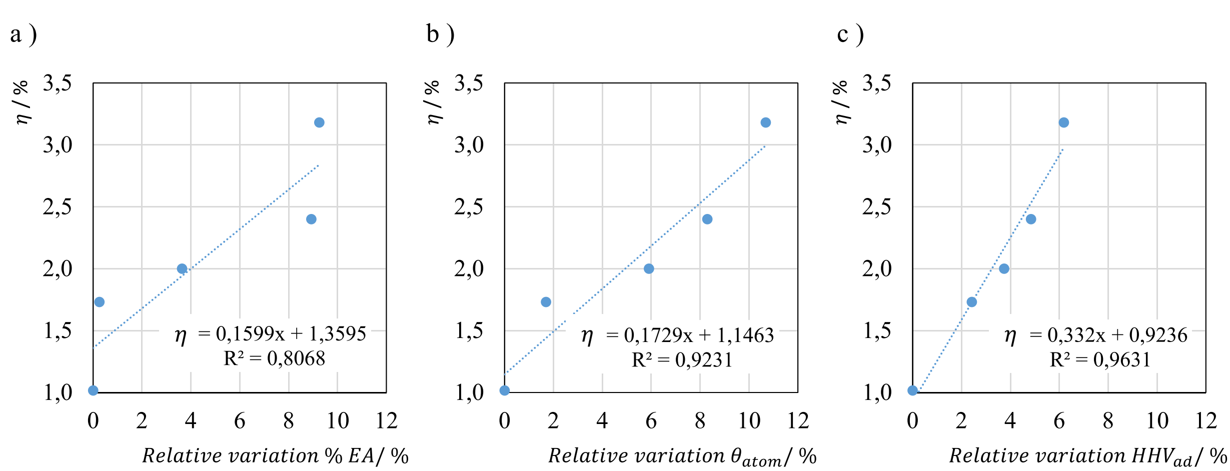

Fig. 5. Scatterplot and lineal regression of η at Idle regime against the relative variation of (a) $\%EA$, (b) θ_{atom}, and (c) HHV_{ad}.

and depicted in Fig. 6. Specifically, the normalized efficiency and acceleration time as functions of the biodiesel content are displayed in Fig. 6a. The normalized efficiency and $\%EA_{norm}$ as functions of the biodiesel content are presented in Fig. 6b. It can be observed from the intersection points of those functions that the optimum trade-off w_{BD} content lays around 15,8% v/v. This content is found to increase the $\%EA$ but avoiding a significant reduction of η and t_{ac}.

Complimentarily to the experimental analyses, the environmental and economic impacts of the palm biodiesel substitution on the Jet A1 operation in the J69 engine can be quantified in terms of the SGE and the SOC, respectively. These results are presented in Fig. 4c. A clear diminishing of SGE is observed against the biodiesel content in the fuel blend, which can be linked to the lower GHG-emissions of the biodiesel. Nevertheless, an SGE raise is observed for a 10% substitution content due to a significant $TSFC$ increase compared with the GHG-emissions reduction. The SOC findings indicate a rise in the operation costs for higher biodiesel contents in the fuel blend, which is related to the higher price of biodiesel in comparison to the Jet A1.

The present findings are coherent with the general literature agreement regarding the aeronautic industry perspectives and challenges of the use of bio-derived aviation fuels [3,47,52,57]. Essentially, the obtained results with null engine modifications indicate a palm oil FAME substitution feasibility in terms of engine performance and environmental impacts. However, extended sustainability analysis forecasts a much more complex future. According to the projections by Janić [58] and Staples et al. [57], only a marginal reduction of the direct GHG-emissions will be affordable by 2050 if a 100% synthetic and biomass-derived fuels substitution of traditional fuels is consummated. The sustainability of biofuels substitution actions is restrained to relevant improvements of the bio-fuel production pathways (including the better land use) and the reduction of the bio-refineries capital cost [58]. Authors like Blakey et al. [52] and Janić [58] also suggest that biofuels like FAME are not suitable to be employed in the aviation sector due to their possibly high metal contamination, their low energy density or the preferred utilization of first-generation biofuels.

At the optimum trade-off biodiesel volume content of 15,8%, the calculated SGE and SOC are 4,6 $kg_{CO_{2,eq}}/N$ per year and 8,5 $MillionUSD/N$ per year, respectively. Thereby, a slight reduction in the environmental impact is projected with a rise of 25% in the operating costs, avoiding significant variations of the engine performance and reducing the evolved CO and HC. The reported values of SGE and SOC can be sharply altered by future market fluctuations, like a crude oil shortage or an aviation transport underuse, following variations in the international fuel prices. In this sense, an average fluctuation of the international fuel price during the last 5 years for the biodiesel and Jet A1 can be estimated in 26,4% and 40,6%, respectively [46]. Moreover, the Willingness To Pay – WTP of the organization and the least-cost travel policies may prevent the commercialization of bio-jet fuel in the coming years [59]. As the uncertainty of this environmental and economic impact is relevant, a more refined analysis is advised for further studies. Even so, the biodiesel substitution scenario is still one of the few immediate and plausible alternatives for the aviation sustainability, mainly due to the chemical properties of the FAME (associated with the H/C ratio of lipid bio-aviation fuels) [60], the existing regulations such as the ASTM D7566 or the DIN EN 14214 standards [61], and the feedstock availability of oil palm that lowers its cost [3]. In order to achieve the globally subscribed targets by 2050, it is fundamental to enable diverse aviation biofuels at a commercial scale [52]. This can only be achieved by boosting the production of liquid hydrogen – LH_2, hydro-processed, and Fischer-Tropsch biofuels [52].

Outstanding findings and visual inspection of the main components of the engine

In addition to the exposed effects of biodiesel on the performance of the engine and the evolved emissions, three outstanding findings are observed during the operation of the J69 engine. The first one is that the utilization of biodiesel above 30% v/v hinders the ignition procedure at the starting of the engine. The second one is an evolution of cloudiness observed at the exhaust gas during the shutdown of the engine for w_{BD} above 20%. The third one is that some components of the combustion chamber are contaminated with soot and unburned matter.

First, during the start-up procedure of the J69 engine, improper functioning of the ignition system is observed when increasing w_{BD}. This malfunctioning occurs for the B30 and B50 blends, particularly when the temperature of the engine is initially below 20 °C. The findings in those tests occur as follows. In the start-up procedure, ω_{shaft} is raised up with the starter-generator and thereupon the fuel nozzle injects the fuel blend. Then, the starting igniter plug is switched on, but no combustion is observed. In consequence, the engine combustor shells are overflowed with fuel and the test is forced to stop. This behavior can be linked to the reduction of the atomization angle of the

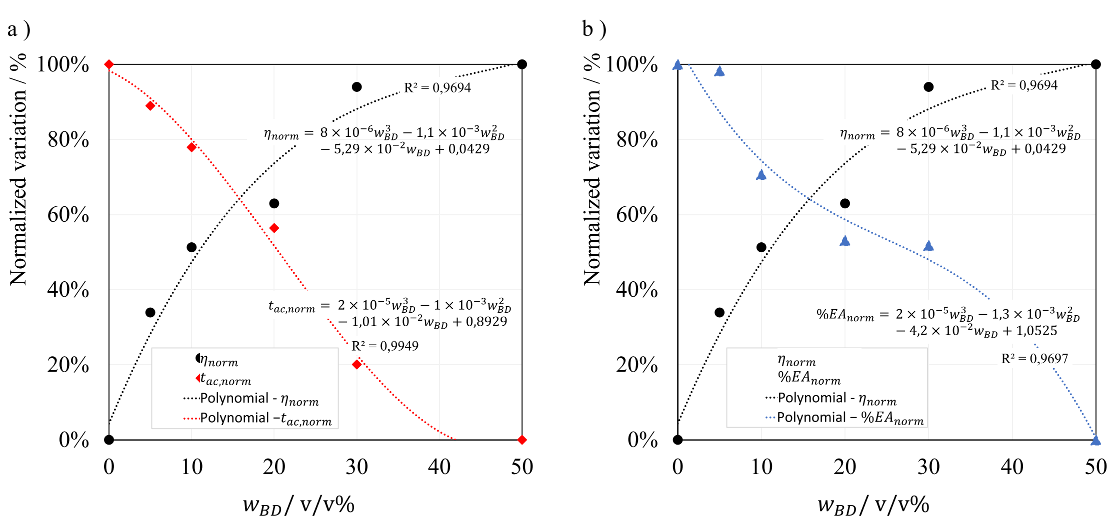

Fig. 6. Variation of the engine performance at Idle in terms of w_{BD}. Profiles of: (a) $t_{ac,norm}$ and η_{norm}, and (b) $\%EA_{norm}$ and η_{norm}. The third order polynomial regressions of each variable are indicated with dotted lines.

Fig. 7. Development of cloudiness in the exhaust gas during the course of the shutdown procedure of the engine. Photographs of the experimental facility during the biodiesel content w_{BD} tests of: (a) B0, (b) B20, and (c) B50.

fuel in the nozzle injectors and the increase of the viscosity of the fuel when the combustion chamber is below 20 °C. According to Pradelle et al. [25], this issue can be mitigated by implementing a pre-heater within the fuel tanks or the injection systems.

Second, significant development of cloudiness is observed in the exhaust gas in the course of the shutdown procedure of the engine, as presented in Fig. 7. This cloudiness appears particularly when w_{BD} is above 20% and the EGT is below 400 °C, which is the temperature that can be reached 2 s after the shutdown started. This behavior has been also reported by French et al [17] and can be associated with the high cetane number of biodiesels or the soot formation dependence upon the fuel pyrolysis [24]. It is noteworthy that a slight amount of fuel is being injected by the fuel distributor during the last seconds of the shutdown procedure, but the biodiesel contained in the fuel blend is not capable of reacting at temperatures below 400 °C, therefore, a raise in the HC and unburned matter production is observed in the exhaust gas. The production of cloudiness during the shutdown procedure can be tackled by reducing the cetane number of the biodiesel and Jet A1 blend using additives. According to Kimble-Thom et al. [20] and Pradelle et al. [25], the utilization of castor oil and n-butanol-based additives containing up to 20% of anhydrous ethanol can reduce the cetane number of biodiesels from 55 to 40.

Third, the improper functioning of the start-up of the engine and the cloudiness during the shutdown procedure caused a contamination of the inner combustor shell, outer combustor shell, and the turbine stator vanes with soot and unburned matter. A graphical depiction of those components is presented in Fig. 8, contrasting their aspect before and after the experimental runs. The foresight of a negative impact on the maintenance routine of the J69 engine is highlighted from this study since the levels of contamination observed in those components after 70 h of operation with biodiesel blends are frequently achieved after 1000 h of operation with the pure Jet A1 [41]. Although the results of the current work enable the evaluation of the biodiesel substitution in terms of the energy performance and the contamination of the main components, a more detailed examination of the mechanical wearing of the engine and its effect on the maintenance program is advised for future studies.

Conclusions

An extended technical analysis has been achieved in the present article of the experimental tests involving an aeronautic J69-T-25A turbojet engine (power rating of 640 kW) and the operation using blends of Jet A1 and palm oil biodiesel up to 50% volume content. The analysis has been focused on the thermal, mechanical, and economic feasibility of the partial biodiesel substitution as operating fuel. Even though the 50% v/v of biodiesel engine operation is achieved without any mechanical adjustment of the engine, an optimum trade-off value

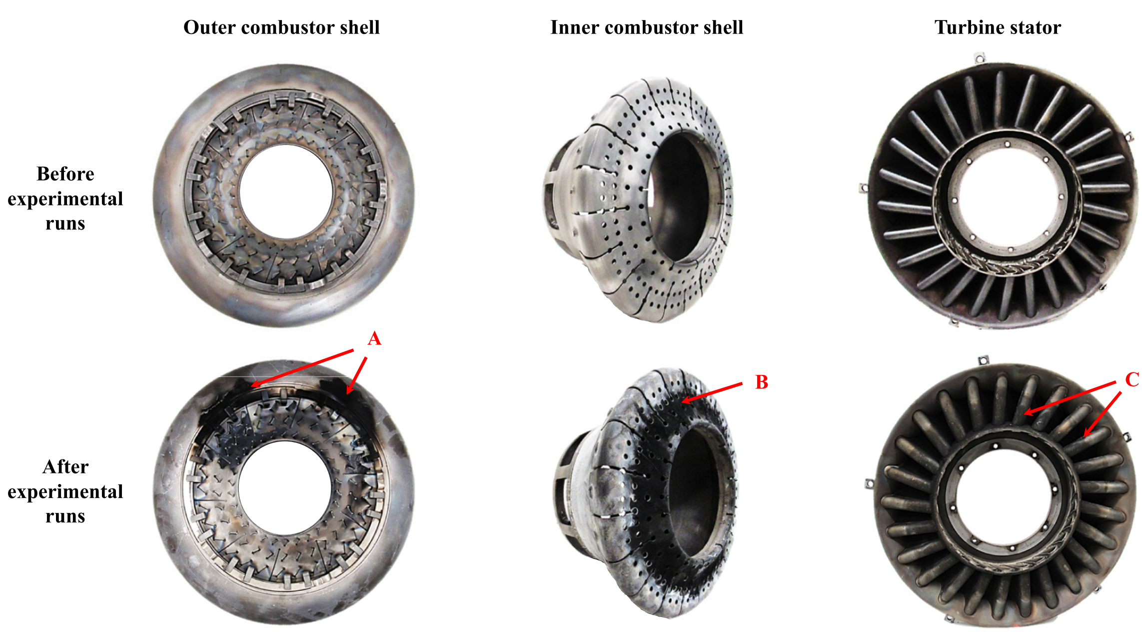

Fig. 8. Visual inspection of the contamination of the turbine stator, and the outer and the inner combustion shells, contrasting their aspect before and after the experimental runs. Photographic details A and B show unburned and oily matter deposition in the combustor chamber. Photographic detail C shows the soot deposition in the vanes of the turbine stator.

of 15,8% biodiesel volume content is advised to avoid significant diminishing of the global energy efficiency – η and the raise in the engine acceleration time – t_{ac}. This value is also motivated by the CO and HC emissions reductions in the exhaust gases. Furthermore, a slight reduction in the GHG-emissions and a raise of 25% in the operating fuel costs are calculated for this trade-off value, which are in agreement with the literature reports regarding the challenges for the employment of bio-derived fuels in the aeronautic industry. The use of biodiesel FAME in the fuel blend gives "the insight" of a complete combustion when increasing w_{BD} as the $\%EA$ raises and the CO and HC emissions diminish. Nevertheless, both the reduction of the HHV_{ad} and the poor atomization, in addition to the higher viscosity and density of the biodiesel seem to promote slower combustion. As a result, the engine efficiency drops by 76,3% in the case of the operation with 50% biodiesel content at Idle.

Regarding the operation ranges and the biodiesel substitution, an overriding influence of the biodiesel content on the engine performance is noticed at Idle, but no significant differences are observed at high loads such as Cruise and Take-off. The employment of w_{BD} above 30% also hinders the ignition at the start-up procedure of the engine and, even more important, some components of the combustion chamber show soot and unburned matter contamination as a result of cloudiness development in the exhaust gas during the shutdown procedure. The present results enable the quantification of the biodiesel substitution effects on the energy performance of a full-size aviation turbine engine. Nonetheless, a more detailed examination of the mechanical wearing of the main components of the engine is advised for further related studies. Although these findings indicate a feasible use of palm oil FAME in aeronautic transport, it is fundamental to diversify the employment of aviation biofuels at the commercial scale in order to achieve the globally subscribed sustainability goals by 2050.

CRediT authorship contribution statement

Gabriel Talero: Conceptualization, Data curation, Formal analysis, Methodology, Writing - original draft, Investigation, Visualization. **Camilo Bayona-Roa:** Formal analysis, Writing - original draft, Writing - review & editing. **Vladimir Silva:** Conceptualization, Project administration, Data curation, Investigation. **Manuel Mayorga:** Investigation, Data curation, Writing - review & editing. **Juan Pava:** Methodology, Project administration. **Mauricio Lopez:** Funding acquisition, Project administration.

Declaration of Competing Interest

The authors declare that they have no known competing financial interests or personal relationships that could have appeared to influence the work reported in this paper.

Acknowledgments

This work was supported and funded by Colciencias (Grant No. 56752), the Colombian Air Force – FAC, the Universidad ECCI and the Universidad Nacional de Colombia. The authors thank Hamilton Henao from CAMAN for all the support during the experimental labor, Professor Nelson Jimenez from ESUFA, Professor Javier Bonilla from the Universidad ECCI and Miguel Galindo, Giovanny Muñoz and Renso Arango. C. Bayona-Roa acknowledges the support of Colciencias through the postdoctoral scholarship.

Appendix A. Supplementary data

Supplementary data to this article can be found online at https://doi.org/10.1016/j.seta.2020.100746.

References

[1] Prussi M, O'Connell A, Lonza L. Analysis of current aviation biofuel technical production potential in EU28. Biomass Bioenergy 2019;130:105371. https://doi.org/10.1016/j.biombioe.2019.105371.

[2] Unglert M, Bockey D, Bofinger C, Buchholz B, Fisch G, Luther R, et al. Action areas and the need for research in biofuels. Fuel 2020;268. https://doi.org/10.1016/j.fuel.2020.117227.

[3] Wang M, Dewil R, Maniatis K, Wheeldon J, Tan T, Baeyens J, et al. Biomass-derived aviation fuels: Challenges and perspective. Prog Energy Combust Sci 2019;74:31–49. https://doi.org/10.1016/j.pecs.2019.04.004.

[4] Kandaramath Hari T, Yaakob Z, Binitha NN. Aviation biofuel from renewable resources: Routes, opportunities and challenges. Renew Sustain Energy Rev 2015;42:1234–44. https://doi.org/10.1016/j.rser.2014.10.095.

[5] Tang NYA, Wu CL, Tan D. Evaluating the implementation of performance-based fuel uplift regulation for airline operation. Transp Res Part A Policy Pract 2020;133:47–61. https://doi.org/10.1016/j.tra.2019.12.028.

[6] Srivastava RK, Shetti NP, Reddy KR, Aminabhavi TM. Biofuels, biodiesel and biohydrogen production using bioprocesses: A review. Environ Chem Lett 2020. https://doi.org/10.1007/s10311-020-00999-7.

[7] Hoxie A, Anderson M. Evaluating high volume blends of vegetable oil in micro-gas turbine engines. Renew Energy 2017;101:886–93. https://doi.org/10.1016/j.renene.2016.09.054.

[8] Habib Z, Parthasarathy R, Gollahalli S. Performance and emission characteristics of biofuel in a small-scale gas turbine engine. Appl Energy 2010;87:1701–9. https://doi.org/10.1016/j.apenergy.2009.10.024.

[9] Mendez CJ, Parthasarathy RN, Gollahalli SR. Performance and emission characteristics of butanol/Jet A blends in a gas turbine engine. Appl Energy 2014;118:135–40. https://doi.org/10.1016/j.apenergy.2013.12.011.

[10] Chuck CJ, Donnelly J. The compatibility of potential bioderived fuels with Jet A-1 aviation kerosene. Appl Energy 2014;118:83–91. https://doi.org/10.1016/j.apenergy.2013.12.019.

[11] Corporan E, Reich R, Larson V, Aulich T, Mann M, Seames W. Impacts of biodiesel on pollutant emissions of a JP-8–fueled turbine engine. J Air Waste Manag Assoc 2005;55:940–9. https://doi.org/10.1080/10473289.2005.10464680.

[12] Nascimento MAR, Lora ES, Corrêa PSP, Andrade RV, Rendon MA, Venturini OJ, et al. Biodiesel fuel in diesel micro-turbine engines: Modelling and experimental evaluation. Energy 2008;33:233–40. https://doi.org/10.1016/j.energy.2007.07.014.

[13] Chiaramonti D, Rizzo AM, Spadi A, Prussi M, Riccio G, Martelli F. Exhaust emissions from liquid fuel micro gas turbine fed with diesel oil, biodiesel and vegetable oil. Appl Energy 2013;101:349–56. https://doi.org/10.1016/j.apenergy.2012.01.066.

[14] Sundararaj RH, Dinesh R, Kumar A, Sekar TC, Pandey V, Kushari A, et al. Combustion and emission characteristics from biojet fuel blends in a gas turbine combustor. Energy 2019;182:689–705. https://doi.org/10.1016/j.energy.2019.06.060.

[15] Udeh GT, Udeh PO. Comparative thermo-economic analysis of multi-fuel fired gas turbine power plant. Renew Energy 2019;133:295–306. https://doi.org/10.1016/j.renene.2018.10.036.

[16] Harahap F, Silveira S, Khatiwada D. Cost competitiveness of palm oil biodiesel production in Indonesia. Energy 2019;170:62–72. https://doi.org/10.1016/j.energy.2018.12.115.

[17] French KW. Recycled fuel performance in the SR-30 gas turbine. Proc 2003 Am Soc Eng Educ Annu. Conf Expo 2003.

[18] Rochelle D, Najafi H. A review of the effect of biodiesel on gas turbine emissions and performance. Renew Sustain Energy Rev 2019;105:129–37. https://doi.org/10.1016/j.rser.2019.01.056.

[19] Rehman A, Phalke DR, Pandey R. Alternative fuel for gas turbine: Esterified jatropha oil-diesel blend. Renew Energy 2011;36:2635–40. https://doi.org/10.1016/j.renene.2010.06.013.

[20] Kimble-Thom MA, Stanley DL, Cholis JT, Lopp DW. The use of bio-fuels as additives and extenders for aviation turbine. Fuels 2014;V002T01A007. https://doi.org/10.1115/99-gt-293.

[21] Chiong MC, Chong CT, Ng JH, Lam SS, Tran MV, Chong WWF, et al. Liquid biofuels production and emissions performance in gas turbines: A review. Energy Convers Manag 2018;173:640–58. https://doi.org/10.1016/j.enconman.2018.07.082.

[22] Lupandin V, Thamburaj R, Nikolayev A. Test results of the OGT2500 gas turbine engine running on alternative fuels: BioOil. BioDiesel and Crude Oil Ethanol 2005:421–6.

[23] Panchasara HV, Simmons BM, Agrawal AK, Spear SK, Daly DT. Combustion performance of biodiesel and diesel-vegetable oil blends in a simulated gas turbine. Burner 2008:377–88.

[24] Kumal RR, Liu J, Gharpure A, Vander Wal RL, Kinsey JS, Gianelli B, et al. Impact of biofuel blends on black carbon emissions from a gas turbine engine. Energy Fuels 2020. https://doi.org/10.1021/acs.energyfuels.0c00094.

[25] Pradelle F, Leal Braga S, de Aguiar Fonseca, Martins AR, Turkovics F, Pradelle Nohra Chaar R. Experimental assessment of some key physicochemical properties of diesel-biodiesel-ethanol (DBE) blends for use in compression ignition engines. Fuel 2019;248:241–53. https://doi.org/10.1016/j.fuel.2019.03.087.

[26] Čerňan J, Hocko M, Cúttová M. Safety risks of biofuel utilization in aircraft operations. Transp Res Procedia 2017;28:141–8. https://doi.org/10.1016/j.trpro.2017.12.179.

[27] Badami M, Nuccio P, Signoretto A. Experimental and numerical analysis of a small-scale turbojet engine. Energy Convers Manag 2013;76:225–33. https://doi.org/10.1016/j.enconman.2013.07.043.

[28] Brem BT, Durdina L, Siegerist F, Beyerle P, Bruderer K, Rindlisbacher T, et al. Effects of fuel aromatic content on nonvolatile particulate emissions of an in-production aircraft gas turbine. Environ Sci Technol 2015;49:13149–57. https://doi.org/10.1021/acs.est.5b04167.
[29] Talero G, Bayona-roa C, Muñoz G, Galindo M, Silva V, Pava J, et al. Experimental methodology and facility for the J69-engine performance and emissions evaluation using Jet al and biodiesel blends. Energies 2019;12:4530. https://doi.org/10.3390/en12234530.
[30] Bayona-Roa C, Solís-Chaves J, Bonilla J, Rodriguez-Melendez A, Castellanos D. Computational simulation of PT6A gas turbine engine operating with different blends of biodiesel – A transient-response analysis. Energies 2019;12:4258. https://doi.org/10.3390/en12224258.
[31] Ali AHH, Ibrahim MN. Performance and environmental impact of a turbojet engine fueled by blends of biodiesels. Int J Environ Sci Technol 2017;14:1253–66. https://doi.org/10.1007/s13762-016-1228-4.
[32] da Silva JQ, Santos DQ, Fabris JD, Harter LVL, Chagas SP. Light biodiesel from macaúba and palm kernel: Properties of their blends with fossil kerosene in the perspective of an alternative aviation fuel. Renew Energy 2020;151:426–33. https://doi.org/10.1016/j.renene.2019.11.035.
[33] Benjumea P, Agudelo J, Agudelo A. Basic properties of palm oil biodiesel-diesel blends. Fuel 2008;87:2069–75. https://doi.org/10.1016/j.fuel.2007.11.004.
[34] Varatharajan K, Pushparani DS. Screening of antioxidant additives for biodiesel fuels. Renew Sustain Energy Rev 2018;82:2017–28. https://doi.org/10.1016/j.rser.2017.07.020.
[35] Pimenidou P, Shanmugapriya N, Shah N. Performance and emissions study of diesel and waste biodiesel blends with nanosized CZA2 of high oxygen storage capacity. Fuel 2019;239:1072–82. https://doi.org/10.1016/j.fuel.2018.11.036.
[36] Amid S, Aghbashlo M, Tabatabaei M, Hajiahmad A, Najafi B, Ghaziaskar HS, et al. Effects of waste-derived ethylene glycol diacetate as a novel oxygenated additive on performance and emission characteristics of a diesel engine fueled with diesel/biodiesel blends. Energy Convers Manag 2020;203. https://doi.org/10.1016/j.enconman.2019.112245.
[37] Yang J, Xin Z, He (Sophia) Q, Corscadden K, Niu H. An overview on performance characteristics of bio-jet fuels. Fuel 2019;237:916–36. https://doi.org/10.1016/j.fuel.2018.10.079.
[38] Hashimoto N, Ozawa Y, Mori N, Yuri I, Hisamatsu T. Fundamental combustion characteristics of palm methyl ester (PME) as alternative fuel for gas turbines. Fuel 2008;87:3373–8. https://doi.org/10.1016/j.fuel.2008.06.005.
[39] Mayorga MA, López M, López CA, Bonilla JA, Silva V, Talero GF, et al. Production of aviation biofuel from palm kernel oil. Chem Eng Trans 2020:80.
[40] Mayorga MA, Cadavid JG, Martínez J, Rodríguez-Varela LI, Trujillo CA, López M, et al. Evaluation of zeolite-based catalyst supports for the production of biokerosene by hydrotreating of oils. Chem Eng Trans 2019;74:13–8. https://doi.org/10.3303/CET1974003.
[41] TELEDYNE CAE. Technichal Manual T.0. 2J-J69-72 Intermediate Maintenance Instructions Turbojet Engine Model No. J69-T-25-A. Secretary of the Air Force; 2004.
[42] Choi S, Lee D, Park J. Ignition and combustion characteristics of the gas turbine slinger combustor. J Mech Sci Technol 2008;22:538–44. https://doi.org/10.1007/s12206-007-1106-6.
[43] Elkelawy M, Bastawissi HAE, Esmaeil KK, Radwan AM, Panchal H, Sadasivuni KK, et al. Maximization of biodiesel production from sunflower and soybean oils and prediction of diesel engine performance and emission characteristics through response surface methodology. Fuel 2020;266:117072. https://doi.org/10.1016/j.fuel.2020.117072.
[44] Moffat RJ. Describing the uncertainties in experimental results. Exp Therm Fluid Sci 1988;1:3–17. https://doi.org/10.1016/0894-1777(88)90043-X.
[45] Talero G, Rincón S, Gómez A. Biomass torrefaction in a standard retort: A study on oil palm solid residues. Fuel 2019;244:366–78. https://doi.org/10.1016/j.fuel.2019.02.008.
[46] U.S. Department of Energy - Energy Efficiency and Renewable Energy. CLEAN CITIES Alternative Fuel Price Report (AFPR) - 2019. Washington, D.C.: 2019.
[47] Wang WC, Tao L. Bio-jet fuel conversion technologies. Renew Sustain Energy Rev 2016;53:801–22. https://doi.org/10.1016/j.rser.2015.09.016.
[48] Sallevelt JLHP, Gudde JEP, Pozarlik AK, Brem G. The impact of spray quality on the combustion of a viscous biofuel in a micro gas turbine. Appl Energy 2014;132:575–85. https://doi.org/10.1016/j.apenergy.2014.07.030.
[49] Sivakumar D, Vankeswaram SK, Sakthikumar R, Raghunandan BN, Hu JTC, Sinha AK. An experimental study on jatropha-derived alternative aviation fuel sprays from simplex swirl atomizer. Fuel 2016;179:36–44. https://doi.org/10.1016/j.fuel.2016.03.050.
[50] Chong CT, Hochgreb S. Flame structure, spectroscopy and emissions quantification of rapeseed biodiesel under model gas turbine conditions. Appl Energy 2017;185:1383–92. https://doi.org/10.1016/j.apenergy.2016.01.003.
[51] Kurji H, Valera-Medina A, Runyon J, Giles A, Pugh D, Marsh R, et al. Combustion characteristics of biodiesel saturated with pyrolysis oil for power generation in gas turbines. Renew Energy 2016;99:443–51. https://doi.org/10.1016/j.renene.2016.07.036.
[52] Blakey S, Rye L, Wilson CW. Aviation gas turbine alternative fuels: A review. Proc Combust Inst 2011;33:2863–85. https://doi.org/10.1016/j.proci.2010.09.011.
[53] Elkelawy M, Etaiw SE, Din H, Bastawissi HAE, Marie H, Elbanna A, Panchal H, et al. Study of diesel-biodiesel blends combustion and emission characteristics in a CI engine by adding nanoparticles of Mn (II) supramolecular complex. Atmos Pollut Res 2020;11:117–28. https://doi.org/10.1016/j.apr.2019.09.021.
[54] Elkelawy M, Alm-Eldin Bastawissi H, Esmaeil KK, Radwan AM, Panchal H, Sadasivuni KK, et al. Experimental studies on the biodiesel production parameters optimization of sunflower and soybean oil mixture and DI engine combustion, performance, and emission analysis fueled with diesel/biodiesel blends. Fuel 2019:255. https://doi.org/10.1016/j.fuel.2019.115791.
[55] Flora G, Balagurunathan J, Saxena S, Cain JP, Kahandawala MSP, DeWitt MJ, et al. Chemical ignition delay of candidate drop-in replacement jet fuels under fuel-lean conditions: A shock tube study. Fuel 2017;209:457–72. https://doi.org/10.1016/j.fuel.2017.07.082.
[56] Chong CT, Hochgreb S. Spray flame structure of rapeseed biodiesel and Jet-A1 fuel. Fuel 2014;115:551–8. https://doi.org/10.1016/j.fuel.2013.07.059.
[57] Staples MD, Malina R, Suresh P, Hileman JI, Barrett SRH. Aviation CO2 emissions reductions from the use of alternative jet fuels. Energy Policy 2018;114:342–54. https://doi.org/10.1016/j.enpol.2017.12.007.
[58] Janić M. An assessment of the potential of alternative fuels for “greening” commercial air transportation. J Air Transp Manag 2018;69:235–47. https://doi.org/10.1016/j.jairtraman.2017.09.002.
[59] Goding L, Andersson-Franko M, Lagerkvist CJ. Preferences for bio jet fuel in Sweden: The case of business travel from a city airport. Sustain Energy Technol Assessments 2018;29:60–9. https://doi.org/10.1016/j.seta.2018.06.015.
[60] O’Connell A, Kousoulidou M, Lonza L, Weindorf W. Considerations on GHG emissions and energy balances of promising aviation biofuel pathways. Renew Sustain Energy Rev 2019;101:504–15. https://doi.org/10.1016/j.rser.2018.11.033.
[61] Mayorga Betancourt MA, Cadavid Estrada JG, Bonilla Paez JA, López Santamaría CA, López Gómez M. Use of Biofuels in the Aeronautical Industry: Colombian Air Force Case. TECCIENCIA 2019;14:53–63. https://doi.org/10.18180/tecciencia.2019.14.7.